G-Gitter Fully Developed Mixed Convection Flow in a Vertical Channel with Suction and Injection

Ahmad K. Samaila[1] and Basant K. Jha[2]

Abstract**—** The effect of g-gitter induced by mixed convection flow in a vertical channel with suction/injection is considered in this paper. The channel walls are maintained at different constant temperatures. The closed form expressions for velocity field, temperature field, skin-friction, and pressure gradient are obtained. Graphical results for the velocity and temperature profiles as well as skin friction and rate of heat transfer are presented and discussed for various parametric physical conditions. The results indicated that presence of suction/injection breaks the symmetry of velocity and temperature fields and also is an effective tool to control the flow reversal.

Keywords**—** g-jitter, mixed convection, suction/injection vertical channel

I. Introduction

CONVECTIVE motion in vertical channels has attracted considerable attention by many authors because of its applications in geophysics, oil recovery technique, and thermal insulation, engineering, and heat storage systems. Natural convection is driven by buoyancy forces resulting from both temperature gradient and gravity field. This convective flow is known to have a profound effect on the solutal homogeniety of crystals grown from melt on earthbound conditions. Much of the interest in going to space to carry out the melt growth semiconductor or metal crystals is to reduce this buoyancy driven convection through significant reduction in gravity. While microgravity environment is indeed helpful in suppressing convective flows, it introduces additional effects that are undetectable or present during Earth-based crystals. One of this effects that affects the melt growth experiments is the flow associated with residual accelerations or g-gitter. Flight experiments unveiled that residual accelerations or g-gitter occurring during space processing can cause appreciable convective flows in the melt pool, making it difficult to realize a diffusion controlled growth from melts in microgravity, as originally intended [1].

Samaila K.. Ahmad[1] is with the Department of Mathematics,Usmanu Danfodiyo University, Sokoto, Nigeria (phone:0803612002 e-mail: ahmadkenga@gmail.com Corresponding author)

Basant K. Jha [2], He is with the Department of Mathematics, Ahmadh Ahmadu Bello University, Zaria,Nigeria. (e-mail: basant777@yahoo.co.uk)

The residual accelerations associated with microgravity come from crew motions, mechanical vibrations (pumps, motors, excitations of natural frequencies of spacecraft structures), spacecraft manoeuvres and attitude, atmosphere drag and the Earth's gravity gradient [2]. Studies on g-gitter effects showed that convection microgravity is related to the magnitude of g-gitter and to the alignment of the gravity field with respect to the growth direction or the direction of the temperature gradient [3-5]. A residual gravity of $10^{-5},10^{-6}g$ is found to be sufficient to cause unacceptable fluid motion in the liquid, unacceptable in the sense that the g-gitter induced flow is intensive enough to affect deleteriously the solutal element distributions in the melt flows. The orientation of the gravity vector with respect to the temperature gradient plays important role in melt flows. The velocity attains a maximum when the gravity vector is perpendicular to the temperature gradient Li [6]. Several attempts have been made to estimate and calculate the effects of time varying g-jitter on the convective flow [7-12]. These calculations are all based on numerical models. Amin [13] has investigated the heat transfer from a sphere immersed in an infinite viscous and incompressible fluid in a zero gravity environment under the influence of g-jitter. She has shown that heat transfer is negligibly small for high-frequency g-jitter but under special circumstances, when the Prandt number is sufficiently high, low frequency g-jitter may play an important role. Li [14], and Chamkha [15] have studied the oscillating free and mixed convection flow driven by g-jitter forces associated with microgravity and magnetic field effect for a system consisting of two parallel plates heated at different temperatures. Chamkha [15] included also the heat generation or absorption term into the energy equation and has considered the cases of isoflux-isothermal, isothermal-isoflux and isoflux-isoflux thermal boundary conditions. It is also worth mentioning the papers done by Ress and Pop [16-18] on the g-jitter induced free convection boundary layer over a vertical flat plate embedded in porous medium and near the stagnation point of a body in a porous medium or in viscous fluid (non-porous medium). All these studies have shed some lights on the basic nature of g-jitter effects and have provided a thrust to device useful mechanisms by which the g-jitter induced convective flows may be suppressed. An extensive overview of the sources of unsteady gravitational accelerations derived from analytical and measurements in the space laboratory engineering models can be found in Gresho and Sani [19]. Most recently, Shu *et al.* [20], Pan *et al.* [21], and Sharidan *et al.* [22] consider the phenomenon of g-jitter in free

convection flows arising from the combined buoyancies due to thermal and chemical species diffusion in a cavity. However to the best of author's knowledge, there is no literature that addresses g-jitter fully developed mixed convection flow in a vertical channel with transpiration (suction/injection).

This study therefore, present an exact analytical solution for the problem of laminar g-jitter mixed convection flow in a vertical channel with suction/injection.

II. Mathematical Formulations

Fig.1 shows g-jitter mixed convection in a vertical channel formed by two infinite vertical parallel porous plates with transpiration. The temperature of both porous plates and the fluid are assumed to be T_0. The porous plates are taken vertically parallel to x' (see in Fig.1). It is assumed that the g-gitter field under consideration is constant and the flow at the entrance also oscillates because of an applied pressure gradient. In addition, the flow is subjected to the suction of the fluid at the same rate from one plate in the channel and at the same rate being injected through the other plate.

The fluid is assumed to be Newtonian and obeys the Boussinesq's approximation. Under the above assumptions the energy and momentum equations in dimensional form are:

$$\frac{\partial u'}{\partial t'}-v_0\frac{\partial u'}{\partial y'}=\upsilon\frac{\partial^2 u'}{\partial y'^2}+g*(t')\beta_T(T'-T_0)-\frac{1}{\rho}\frac{\partial p'}{\partial x'} \quad (1)$$

$$\frac{\partial T'}{\partial t'}-v_0\frac{\partial T'}{\partial y'}=\alpha\frac{\partial^2 T'}{\partial y'^2} \quad (2)$$

The initial and boundary conditions to be satisfied are:

$$u'=0,\ T'=T_1 \quad at\ y'=0$$
$$u'=0,\ T'=T_2 \quad at \quad y'=h \quad (3)$$

Where the non-dimensional variables are defined as

$$y=\frac{y'}{h},t\frac{t'v}{H^2},u=\frac{u'}{u_0},T=\frac{(T'-T_0)}{(T_2-T_0)},\gamma_T=\frac{(T'-T_0)}{(T_2-T_0)},\Omega=\frac{h^2\omega'}{\upsilon},s=\frac{v_0h}{\upsilon},\mathrm{Re}=\frac{u_0h}{\upsilon},\mathrm{Pr}=\frac{\upsilon}{\alpha} \quad (4)$$
$$X=\frac{x'}{h},P=\frac{p'h}{U_0\upsilon\rho},g(t)=\frac{g*(t')}{g_0},g*(t')=g_0\sin(\omega' t'),Gr=\frac{g_0\beta_T(T_2-T_0)h^2}{\upsilon^2}$$

Using the expressions (4) in (1) and (2) the dimensionless momentum and energy equations are

$$\frac{\partial u}{\partial t}-s\frac{\partial u}{\partial y}=\frac{\partial^2 u}{\partial y^2}+g(t)\frac{Gr}{\mathrm{Re}}T-\frac{\partial P}{\partial X} \quad (5)$$

$$\frac{\partial T}{\partial t}-s\frac{\partial T}{\partial y}=\frac{1}{\mathrm{Pr}}\frac{\partial^2 T}{\partial y^2} \quad (6)$$

While the initial and boundary conditions in dimensionless form are

$$u=0,T=\gamma_T \quad at\ y=0$$
$$u=0,T=1 \quad at\ y=1 \quad (7)$$

To solve equations (5) and (6), we assume that $g(t)=\sin(\Omega t)$ and use the method of superposition namely, that,

$$U(y,t)=E(y)\exp(i\Omega t)$$
$$P(X,t)=F(X)\exp(i\Omega t) \quad (8)$$

Using Eqs.(5) and (6) we get the temperature and velocity expressions as

$$T(y)=\frac{R_T\left[\exp(-s\,\mathrm{Pr}\,y)-\exp(-spr)\right]}{\left[1-\exp(-spr)\right]}+\frac{\left[1-\exp(-s\,\mathrm{Pr}\,y)\right]}{\left[1-\exp(-s\,\mathrm{Pr})\right]} \quad (10)$$

$$E(y)=\left(\frac{sh(s(1-y)}{sh(\delta)}\right)\left[\frac{1}{\beta^2}\frac{dF}{dx}+\frac{Gr}{\mathrm{Re}}X_5\right]-\frac{1}{\beta^2}\frac{dF}{dx}\left[1-\frac{sh(\delta y)}{sh(\delta)}\exp(-\frac{sy}{2})\exp(\frac{s}{2})\right]$$
$$+\frac{Gr}{\mathrm{Re}}X_6\frac{sh(\delta y)}{sh(\delta)}\exp(-\frac{sy}{2})\exp(\frac{s}{2})+\frac{Gr}{\mathrm{Re}}C_2 \quad (11)$$
$$-\frac{Gr}{\mathrm{Re}}\frac{C_1\exp(-s\,\mathrm{Pr})}{X_1}$$

The skin friction and rate of heat transfer at the boundaries are expressed as

$$\tau_0=\left.\frac{\partial E}{\partial y}\right|_{y=0}=-\frac{s}{2}D_1+\delta D_2+\frac{Gr}{\mathrm{Re}}\frac{s\,\mathrm{Pr}\,C_1}{X_1} \quad (12)$$

$$\tau_1=\left.\frac{\partial E}{\partial y}\right|_{y=1}=-\frac{s}{2}\exp(-\frac{s}{2})\left[D_1ch(\delta y)+D_2sh(\delta y)\right]$$
$$+\delta\exp(-\frac{s}{2})\left[D_1sh(\delta y)+D_2ch(\delta y)\right] \quad (13)$$
$$+\frac{Gr}{\mathrm{Re}}\frac{C_1s\,\mathrm{Pr}\exp(-s\,\mathrm{Pr})}{X_1}$$

$$Nu_0=\left.\frac{dT}{dy}\right|_{y=0}=\frac{\gamma t(-s\,\mathrm{Pr})}{1-\exp(-s\,\mathrm{Pr})}+\frac{s\,\mathrm{Pr}}{1-\exp(-s\,\mathrm{Pr})} \quad (14)$$

$$Nu_1=\left.\frac{dT}{dy}\right|_{y=1}=\frac{\gamma t(-s\,\mathrm{Pr}\exp(-s\,\mathrm{Pr})}{1-\exp(-s\,\mathrm{Pr})}+\frac{s\,\mathrm{Pr}\exp(-s\,\mathrm{Pr})}{1-\exp(-s\,\mathrm{Pr})} \quad (15)$$

and $\delta, D_1, D_2, X_1, X_2, X_3.....X_{24}$ are defined in the appendix

III. Results And Discussion

Analytical solution given by Eqs. (10) and (11) are illustrated in figs. 2 to 19 for some values of the physical parameters involved. Fig.2 displays typical velocity profiles in vertical parallel porous plates for different values of suction/injection parameter (s). The velocity field depend on suction/injection parameters s and Ωt. It is seen from the figure that velocity increases with time. This figure also reflects that when suction takes place on the porous plate at $y=0(s>0)$ fluid velocity is higher compared to a situation when injection takes place on the porous plate at $y=0$ $(s<0)$. This is physically true since suction on the porous plate $y=0$ happens concurrently with injection on the moving porous plate $(y=1)$ which acts in supports of the motion of the porous plate $(y=1)$ and hence an increase in fluid velocity is the consequence. In addition, in case of suction velocity is maximum near the left plate $(y=0)$ and in case of injection the maximum is shifted near the right plate $(y=1)$ and hence we conclude that there is no symmetry in the velocity profile in the presence of suction/injection. Very interesting result can be seen in figs. 3, 4, 5 and 6. Fig. 3 shows the effect of Ωt on the velocity profile. At $\Omega t=\pi$ the flow oscillates about zero and changes direction along the width of the channel parabolically. Fig. 4 shows the flow distribution across the channel width which also oscillate about zero. It is observed that there is only a small reversal flow close to the left wall $(y=0)$ but the flow reversal increases after the centerline $y=0$ as s increases. The effect of Ωt on the velocity profile is depicted in figures 5 and 6. These two

figures indicated that velocity is maximum near the right wall $y=1$. Fig.6 shows a well defined wave oscillation along $y-$direction and there exist a nodal point at $y=0.5$ when the velocity is equal to zero. Fig.7 displays temperature profile for different values of s and $\Pr=0.71, \Omega t=\frac{\pi}{2}, \gamma t=0.2, Gre=20$. This figure reveals that as time increases the temperature increases along the channel diagonal. It is also seen from this figure that, there is full reverse flow for some values of Ωt. The effect of suction/injection parameter on the skin friction is presented in figs. 8 to 15 for Ωt between $\frac{\pi}{4}$ to π. At $y=0, \Omega t=\frac{\pi}{4}$ for positive s the skin friction decreases and for negatives s the skin friction increases (figs. 8 and 9) but at $\Omega t=\pi$ the skin friction increases as s increases and decreases as s increases (figs. 10 and 11).On the boundary $y=1$ and $\Omega t=\frac{\pi}{4}$ skin friction increases with the increase of s and decreases with the decrease of s (figs. 12 and 13). Figs. 14 and 15 show the effect of s and Ωt on the skin friction at $y=1$. These two figures reflect that as suction/injection increases the skin friction decreases. The rate of heat transfer, which is expressed as Nusselt number (Nu) at $y=0$ and $y=1$ is shown in figs. 16, 17, 18 and 19. Figure 16 shows a monotonic increase in the rate of heat transfer as suction/injection parameter (s) increases and the rate of heat transfer decreases as suction/injection parameter (s) increases (fig.17). At $y=1$ and $\Omega t=\pi$ for positive s there is an increase in the rate of heat transfer as shown in figure 18 and for negative s the rate of heat transfer increases as s increases (fig. 19).

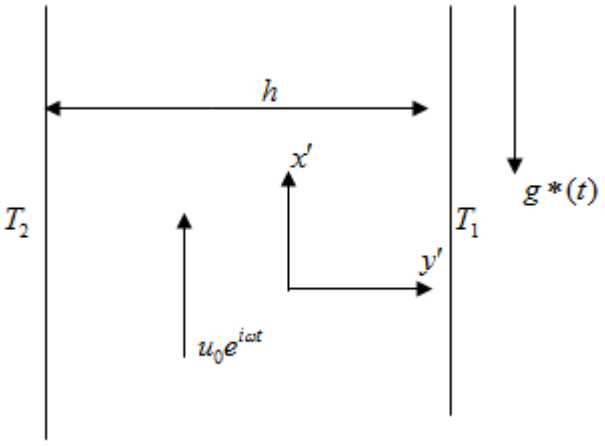

Fig. 1 Physical model and coordinate system

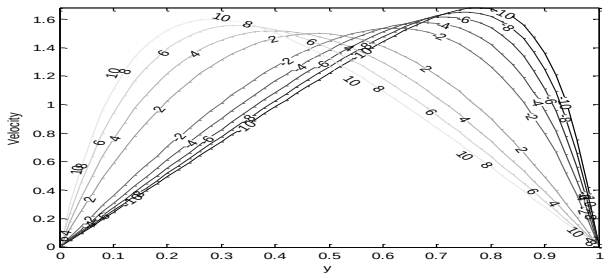

Fig.2 Effects of Ωt on velocity profile

$$\Pr=0.71, \Omega t=\frac{\pi}{2}, \gamma t=0.2$$

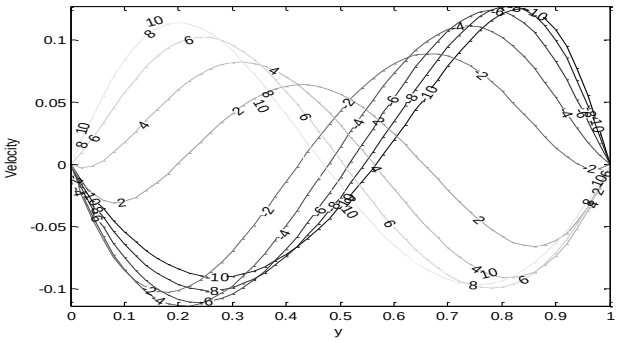

Fig.3 Effects of Ωt on velocity profile

$$\Pr=0.71, \Omega t=\pi, \gamma t=0.2$$

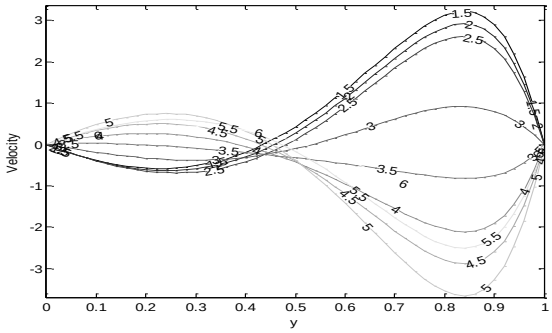

Fig.4 Effects of Ωt on velocity profile for

$$\Omega t=\pi, s=-0.5, \Pr=0.71, Gre=500, \gamma t=0.2$$

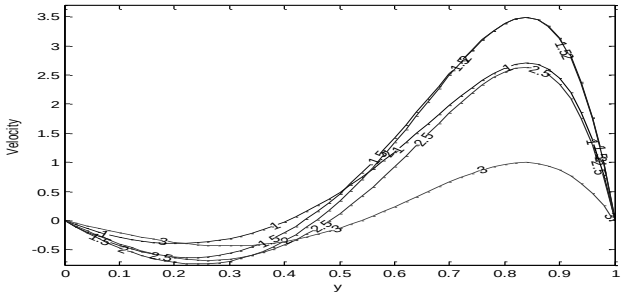

Fig. 5 Effects of Ωt on velocity profile

$$s=-0.5, \Pr=0.71, \Omega t=\frac{\pi}{2}, \gamma t=0.2, Gre=500$$

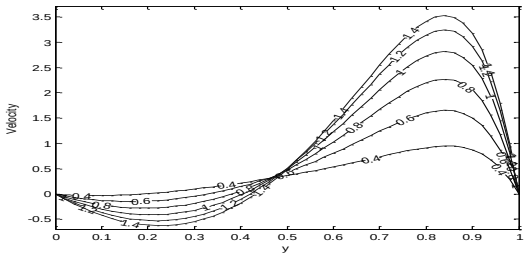

Fig. 6 Effect of Ωt on velocity profile

$s = -0.5, \Pr = 0.71, \Omega t = \frac{\pi}{4}, \gamma t = 0.2, Gre = 500$

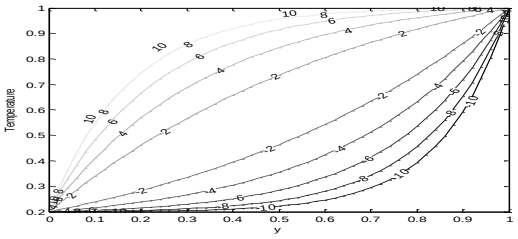

Fig.7 Temperature profile $\Pr = 0.71, \Omega t = \frac{\pi}{2}$

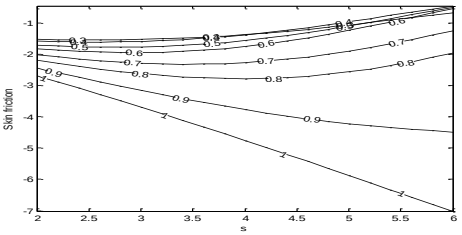

Fig.8 Skin-friction at $y = 0$ and $\Omega t = \frac{\pi}{4}$

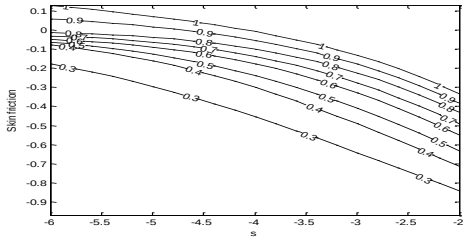

Fig.9 Skin friction $y = 0$ and $\Omega t = \frac{\pi}{4}$

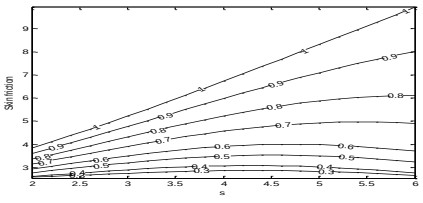

Fig.10 Skin friction at $y = 0$ and $\Omega t = \pi$

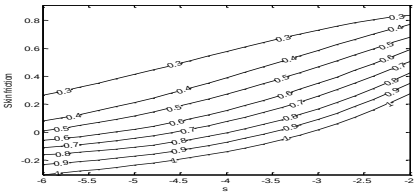

Fig.11 Skin friction at $y = 0$ and $\Omega t = \pi$

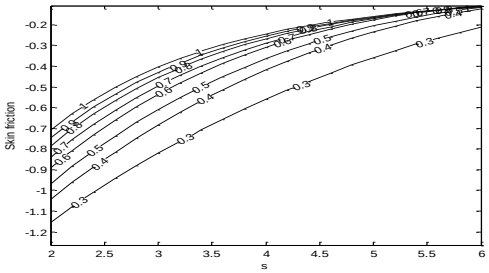

Fig.12 Skin friction at $y = 1$ and $\Omega t = \frac{\pi}{4}$

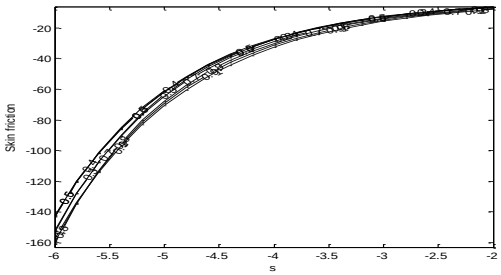

Fig.13 Skin friction $y = 1$ and $\Omega t = \frac{\pi}{4}$

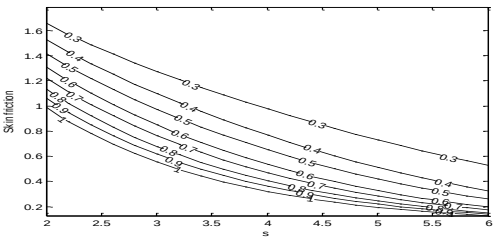

Fig.14 Skin friction at $y = 1$ and $\Omega t = \pi$

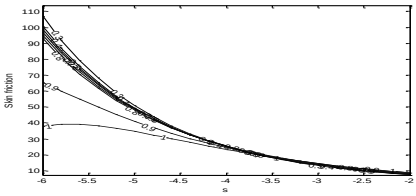

Fig.15 Skin friction $y = 1$ and $\Omega t = \pi$

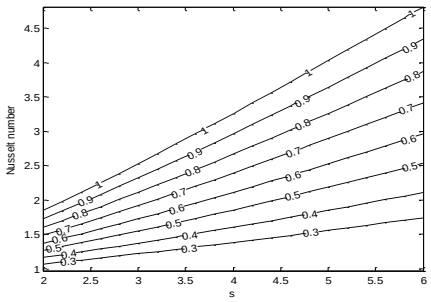

Fig.16. Nusselt number $y = 0, \Omega t = \frac{\pi}{2}$

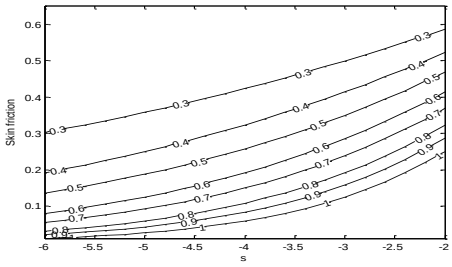

Fig.17 Nusselt number $y = 0, \Omega t = \frac{\pi}{2}$

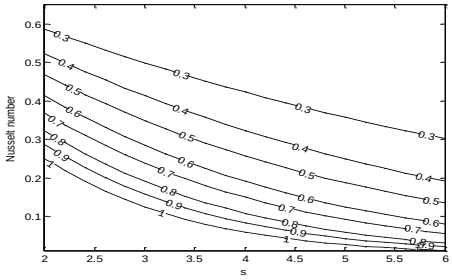

Fig.18 Nusselt number $y = 1, \Omega t = \frac{\pi}{2}$

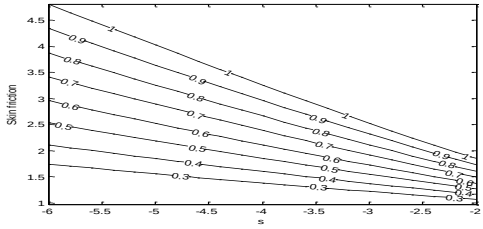

Fig.19 Nusselt number $y = 1, \Omega t = \frac{\pi}{2}$

APPENDIX

Nomenclature:

g - acceleration due to gravity

h - gap between the porous plates

p' - dimensional pressure

P - dimensionless pressure

$\Pr$ - Prandtl number

Re - Reynolds number

v_0 - suction/injection velocity

s - dimensionless velocity

t' - dimensional time

t - dimensionless time

T' - dimensional temperature of the fluid

T_0 - temperature of the fluid at $t' = 0$

u' - dimensional velocity of the fluid

u - dimensionless velocity of the fluid

x' - dimensional co-ordinate parallel to the vertical parallel plates

x - dimensionless co-ordinate parallel to the vertical porous plates

y' - dimensional co-ordinate perpendicular to the channel

y -dimensionless co-ordinate perpendicular to the channel

T - dimensionless temperature of the fluid

Gr - Grashof number

Greek letters

β - volumetric coefficient of thermal expansion

ρ - density of the fluid

τ_0 - dimensionless skin-friction at y=0

τ_1 - dimensionless skin friction at $y = 1$

α - thermal diffusivity

ν - kinematic viscosity

Ω - frequency of g-gitter field

$$C_1 = \frac{[\gamma_T - 1]}{[1-\exp(-s\,\mathrm{Pr})]}, C_2 = \frac{[1-\gamma_T \exp(-s\,\mathrm{Pr})]}{[1-\exp(-s\,\mathrm{Pr})]}, \delta = \sqrt{\frac{s^2}{4}+\beta^2}, \beta = \sqrt{i\Omega}$$

$$X_1 = \left[(s\,\mathrm{Pr})^2 - s^2\,\mathrm{Pr} - \beta^2\right], X_2 = \frac{C_1 s\,\mathrm{Pr}\exp(-s\,\mathrm{Pr})}{X_1}, X_3 = -\frac{1}{\beta^2}C_2, X_4 = -\frac{C_1}{X_1}$$

$$X_5 = X_3 - X_4, X_6 = -\frac{1}{\beta^2}C_2 + \frac{C_1\exp(-s\,\mathrm{Pr})}{X_1}, X_7 = \frac{ch(\delta)}{sh(\delta)}, X_8 = \frac{\exp(s/2)}{sh(\delta)},$$

$$X_9 = X_3 - X_4, X_{10} = X_8 - X_7, X_{11} = X_6 X_8 - X_5 X_7, X_{12} = 1 + X_{10}$$

$$X_{13} = X_9 + X_{11}, X_{14} = 1 - X_{10}, X_{15} = X_9 - X_{11}, X_{16} = \frac{\left[\exp(\delta - s/2) - 1\right]}{(\delta - s/2)}, X_{17} = \frac{\left[\exp\left(-(\delta + s/2) - 1\right)\right]}{(\delta + s/2)}$$

$$X_{18} = \frac{C_1}{X_1}\frac{[\exp(-s\,\mathrm{Pr}) - 1]}{s\,\mathrm{Pr}}, X_{19} = C_2 + NC_4, X_{20} = X_{12}X_{16} - X_{14}X_{17}, X_{21} = X_{13}X_{16} - X_{15}X_{17}$$

$$X_{22} = X_9 ch(\delta) + X_{11} sh(\delta)\left\{\frac{s}{2}\exp(-s/2) + X_2\right\}, X_{23} = \frac{s}{2}\exp(-s/2)\frac{1}{\beta^2}\frac{dF}{dX}(ch(\delta) - X_{10} sh(\delta))$$

$$D_1 = \frac{1}{\beta^2}\frac{dF}{dx} + \frac{Gr}{\mathrm{Re}}X_9, D_2 = \frac{1}{\beta^2}\frac{dF}{dX}X_{10} + \frac{Gr}{\mathrm{Re}}X_{11}$$

REFERENCES

[1] S.Lehoczky, F.R... Szofran, and D.C.Gillies, (1994), Growth of solid solution single crystals. Second United States Microgravity Payload. Six month Science Report, NASA MSC

[2] B.N.Antar, and V.S. Nuotio-Antar, (!993), Fundamentals of Low Gravity Fluid Dynamics and Heat Transfer. CRC Press Boca Raton, FL

[3] J.I.Alexander, (1981), Analysis of the low gravity tolerance of Bridgman Stockbarger crystal growth-II. Steady and impulse accelerations. Microgravity Sci. Technol. 7, 131

[4] J.I.D.Alexander, S.Amiroudine, J. Quazzani, and F.Rosenberger, (1991), Analysis of the low gravity tolerance of Bridgman-Stockbarger crystal growth-II. Transient and periodic accelerations J. Crystal Gowth 113, 21

[5] E.S.Nelson, (1991), An examination on anticipated gittter on space station and its effects on materials processes. NASA TM 103775.

[6] B.Q.Li, (1996), g-gitter induced free convection in a traverse magneticfield.Int J. Heat Mass Transfer. 39(14), 2853-2860.

[7] D.Jacqmin, (1990), Stability of an oscillating fluid with auniformdensitygradient, J. Fluid Mech, 219, 449

[8] W.Zhang, J. Casademunt, J.Venals. and R.F.Sekerka, (1993), Stability of a fluid surface in a microgravity environment. AIAAJI 31 (11), 2027

[9] J.Casademunt, W. Zhang, J.Venals, (1993), Study of the parametric oscillator driven by narrow-band noise to model the response of a fluid surface to time-dependent accelerations, J. Phys. Fluids A 5, 3147.

[10] A.A.Wheeler, G.B.McFadden, B.T.Murray, and S.R. Coriel,(1991), Convective stability in the Rayleigh-Benard and directional solidification problems: high frequency gravity modulation, J. Phys. Fluids A 3, 2847.

[11] J.I.D.,Alexander, (1994), Residual gravity effects on fluid processes, Microgravity Sci. Technol. 2,131.B.Chen, M.H. Saghir, D.H.H. Quon, and S.Chehab, (1994), Numerical study on transient convection in float zone induced by g-gitter, J. Crystal Growth, 142, 362.

[12] N.Amin, (1988), Proc.R.Soc. London.A419 151

[13] B.Q.Li, (1996), Int. J. Eng. Sci., 34, 1369

[14] A.J. Chamkha, (2003), Heat Mass Transfer, 39, 553. Pop, and D.A.S.Rees, (2000), Int. Commun. Heat Mass Transfer, 27, 415

[15] Pop, and D.A.S.Rees, (2001), Int. J. Heat Mass Transfer, 44, 877.

[16] Pop, and D.A.S.Rees, (2001), Heat Mass Transfer, 37,403.

[17] P.M. Gresho, and R.L.Sani, (1970), J. Fluid Mech. 40, 783

[18] Y.Shu, B.Q. Li, and H.C.de Groh, (2001),Numer. Heat Transfer, B Appl.39, 245.

[19] B.O.Pan, B.O.Shang, B.Q. XLi, and H.C.,De Groh, (2002), Int. J. Heat Mass Transfer, 45, 125.

[20] S. Sharidan,.N.Amin, and I.Pop, ((2005), G-gitter fully developed combined heat and mass transfer by mixed convection flow in a vertical channel. Int. Commun. In Heat and Mass Transfer, 32, 657-665.umer Heat Transfer, B Appl. 39, 245

[21] O.Pan, B.O.Shang, B.Q. XLi, and H.C.,De Groh, (2002), Int. J. Heat Mass Transfer, 45, 125. S. Sharidan,.N.Amin, and I.Pop, ((2005), G-gitter fully developed combined heat and mass transfer by mixed convection flow in a vertical channel. Int. Commun. In Heat and Mass Transfer, **32**, 657-665.